

MODELING THE DISTURBANCES AND DYNAMICS OF THE NEW MICRO CT STATION FOR THE MOGNO BEAMLINE AT SIRIUS/LNLS

G. S. Baldon*, G. S. de Albuquerque†, F. Ferracioli, G. B. Z. L. Moreno, R. R. Gerales
 Brazilian Synchrotron Light Laboratory (LNLS), CNPEM, Campinas, Brazil

Abstract

At the 4th generation synchrotron laboratory Sirius at the Brazilian Synchrotron Light Laboratory (LNLS), MOGNO is a high energy imaging beamline, whose Nano-Computed Tomography (CT) station is already in operation. The beamline's 120 nm × 120 nm focus size, 3.1 mrad × 3.1 mrad beam divergence, and 9×10^{11} ph/s flux operated at 21.5 keV, 39.0 keV, and 67.7 keV energies, allow experiments with better temporal and spatial resolution than lower energy and lower stability light sources. To further utilize its potential, a new Micro-CT station is under development to perform experiments with 0.5 μm – 55 μm resolution, and up to 4 Hz sample rotation. To achieve this, a model of the disturbances affecting the station was developed, which comprised: i) the characterization and simulation of disturbances, such as rotation forces; and ii) the modeling of the dynamics of the microstation. The dynamic model was built with the in-house developed Dynamic Error Budgeting Tool, which uses dynamic substructuring to model 6 degrees of freedom rigid body systems. This work discusses the trade-offs between rotation-related parameters affecting the sample-to-optics stability and the experiment resolution in the frequency domain integrated up to 2.5 kHz.

INTRODUCTION

The MOGNO beamline [1] is the hard x-ray micro- and nano-computed tomography (CT) beamline at Sirius, the 4th generation synchrotron light source at the Brazilian Synchrotron Light Laboratory (LNLS). As illustrated in Fig. 1, the beam is generated at a dipole, passes through a slit, and is primarily focused in the horizontal plane with an elliptical mirror (M1). Next, the beam's focus size (120 nm × 120 nm) and position, 3.1 mrad conical divergence, and energy (21.5 keV, 39.0 keV, and 67.7 keV), is finally achieved through a Kirkpatrick-Baez (KB) mirror system, with two stripes and multi-layer coating (Tungsten and Boron Carbide), which allows the beam to reach the sample with a photon flux of 9×10^{11} ph/s. The main detector of the beamline is a PiMega 135D [2], located 27 m away from the focus, which delivers a maximum frame rate of 2×10^3 fps with a 85 mm × 85 mm sensor consisting of a 1536 × 1536 pixel array.

The sample may be at one of the two experimental stations of the beamline: the nanostation, currently under commissioning; or at the microstation, now under construction, and whose error budget is the main subject of this work. Both take advantage of the high photon flux and high frame rate

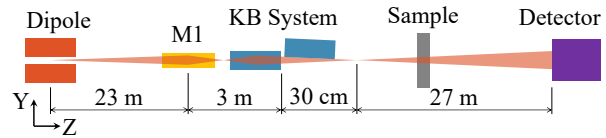


Figure 1: The MOGNO beamline layout. Approximate distances. Z is parallel to the beam, and Y is the vertical upwards.

of the detector to execute time-resolved CT scans, where they can be acquired periodically to observe transient phenomena in in-situ experiments, such as flow through porous media. The time resolution for the nanostation is limited at 5 s, and, for the microstation, at 0.5 s. Additionally, both stations were designed to allow high-throughput CT scans, where the samples are exchanged by a robot without the need of the researcher doing it manually, which greatly improves the speed of experiments with large batches.

The main difference between the stations is the resolution and field of view (FOV): the nanostation was designed to perform CT scans at higher resolution at the cost of smaller FOV and smaller sample sizes. Its sample stage allows movement on a 7 m-long granite rail along the beam direction, resulting in experiments that can range from 120 nm to 13 μm resolution and from 150 μm to 20 mm FOV; the microstation will have a 30 m-long rail, resulting in resolutions between 500 nm and 55 μm, and from 800 μm to 85 mm FOV.

In this work, the objective is the development of a model to analyze the disturbances and the error budget of the microstation. As source and detector stabilities have been designed to meet the more demanding requirements of the nanostation, the main source of error for the microstation is the vibration of the sample itself.

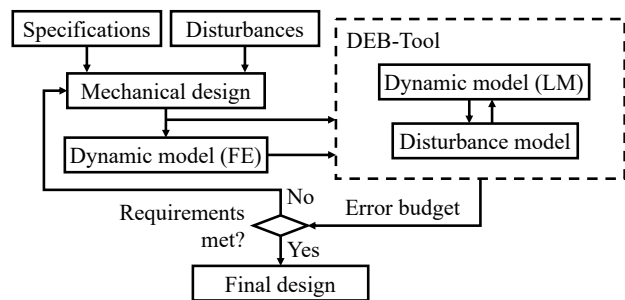


Figure 2: The specifications and disturbances are boundary conditions to the design, which is iterated to meet the requirement, attested through models. Here, FE means finite element, and LM means lumped mass. Adapted from [3].

* gabriel.baldon@lnls.br
 † guilherme.sobral@lnls.br

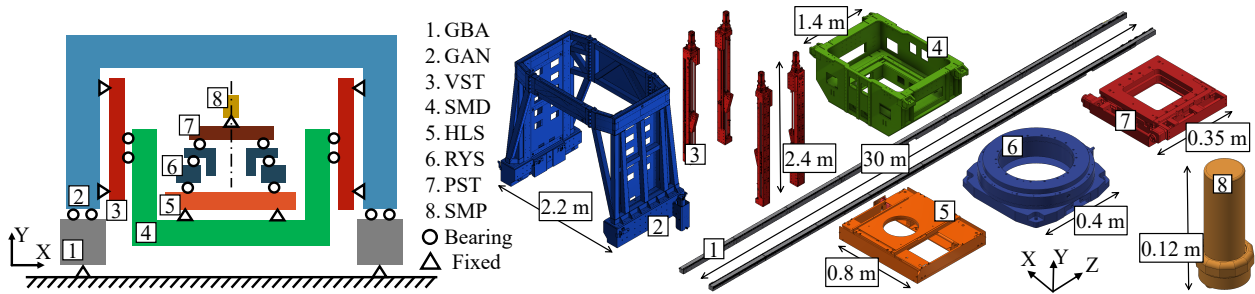


Figure 3: On the left is a schematic of the design of the microstation. And on the right are the detailed parts illustrated in the schematic.

METHODOLOGY

The methodology followed in this work can be summarized with the schematic shown in Fig. 2. This work starts with the mechanical design, which involves the conceptual and detailed design of the system. In this work, the detailed design is important for the disturbance models, as it provides crucial information about the geometry and inertia of system components, improving the fidelity of the model [3].

The dynamic model serves as an ideal representation of the system's dynamics. Two methods are employed for this purpose: finite element (FE) software ANSYS and a lumped mass (LM) approach using the in-house developed DEB-Tool (Dynamic Error Budgeting Tool). The FE-based models provide high accuracy results, but are computationally intensive. While LM models, which fundamentally represent rigid bodies, are much more efficient, and can generate results without the need of a detailed design, but require adjustments to account for flexibility.

At LNLS's beamline engineering teams, FE models are used discerningly. In most cases, an FE model of the complete system is impractical, so these are mostly used to model subsystems to feed information for the LM models. Here, the FE model serves as a high-fidelity reference, guiding adaptations to tune the LM model within DEB-Tool, which is the primary model for aiding the iterative design process.

The tuning of the LM model is done by dividing bodies into smaller parts to represent their flexibility, and is aided by looking at the mode shapes generated with the FE model. The results of such tuning are deemed good when the differences in eigenfrequency between the LM and the FE models are within 5% for the first five eigenmodes.

Both FE models on ANSYS and the LM models on DEB-Tool can use power spectral density (PSD) curves as input to model disturbances, but in this work only DEB-Tool is used for vibration propagation. The input PSDs can be in terms of force, acceleration, velocity or displacement, and with a complete dynamic model, these inputs can return an output PSD on any node of the model. Here, the disturbances considered are two: the floor vibration, with a displacement PSD, and the rotating unbalance, with a force PSD.

Besides the vibration results from the dynamic model, the error budget includes the spindle error motion, which is how the rotational motion of the sample deviates from a

perfect Ry spin. The total combination of these errors must be within a specified limit, and if this requirement is not met, design changes must be made. For the microstation, the limit depends on the resolution of the image, so the critical value is 500 nm peak-to-peak.

MECHANICAL DESIGN

Following the methodology described in the previous section, the microstation design was iteratively changed along the design phase. In its current stage, the station is divided into two gantries, one for sample positioning and the other for supporting auxiliary systems, e.g., the high-throughput module. This allows each gantry to be designed independently, focusing on their different requirements: stiffness, stability, and repeatability for the sample positioning gantry; and structural integrity for the other gantry. A simplified schematic of the sample positioning structure (focus of this work) and its detailed parts are shown in Fig. 3.

A 30-m-long granite base (GBA) coupled with two different mechanisms, granite airpads and linear guides, allows the movement of the microstation along the Z direction. Granite airpads offer repeatability when moving and high stiffness when static [4], and linear guides are used when transitioning between the 3 m-long granite beams that compose the GBA. The movement is actuated using a servo motor with a rack and pinion mechanism attached to the side of the base.

The gantry (GAN) is the trapezoidal steel frame structure that supports four vertical stages (VST) responsible for vertical sample movement, utilizing linear guides and independent servo motors for actuation.

The sample module (SMD) holds a stack of mechatronic stages for sample positioning and rotation, and it is kinematically mounted to the VST with canoe-balls [5]. The horizontal long stroke stage (HLS) provides a 300 mm range for sample positioning. Atop the HLS is the rotational stage (RST), a commercial item by Physik Instrumente (PI) with high precision air bearings, enabling infinite rotation and high-speed operation (up to 7 Hz).

A planar stage (PST) aligns the sample with the RST's rotation axis, offering a range of ± 24 mm, allowing for high-resolution imaging of regions near the sample edge and enabling helical CT scans for noise reduction [6]. However, the PST introduces load unbalance on the RST, which is

addressed by an autobalancing system currently under development by MI-Partners, a Dutch precision engineering firm. The disturbances modeled here consider the microstation with and without the autobalancing system.

DYNAMIC MODEL

As described previously, the dynamic model is done here with two methods: FE and LM.

Finite Element Model

The finite element model was developed in ANSYS Mechanical. It uses the CAD model as input, with simplifications to the geometry, eliminating small holes, fillets, chamfers, and other features that do not affect structural performance but require a finer mesh. Contact between bodies is modeled with the contact stiffness function, and the stiffness values follow empirical data gathered at LNLS from previous projects.

Lumped Mass Model

In the CAD software the bodies are subdividing according to the results of the FE model. From that, the parameters for DEB-Tool, including position of disturbance sources, are automatically exported with Inventor Export Tool (IET), an in-house VBA script developed for this purpose. In DEB-Tool, each connection between bodies is modeled as an elastic support with proportional damping. Figure 4 shows the resulting LM model.

The stiffness of each elastic support is iteratively tuned to match the mode shapes of the FE model, and its initial values are either estimated analytically, or come from experimental data. The results of the modal analysis after this process can be found in Table 1, showing the eigenfrequencies found with each model (LM and FE), and the error between them.

DISTURBANCES

With the dynamic model in DEB-Tool in agreement with the FE model, the next step is to introduce the disturbances and estimate the output errors. The two disturbances modeled were the floor vibration and the rotational unbalance.

Table 1: Modal Analysis Results with FE and LM Models

Mode	Mode shape	f [Hz]		Error [%]
		LM	FE	
1	Rz	26	25.9	-0.3
2	Rx	35.1	36.1	3
3	Rx	49	48.2	-2
4	Ry	53	54.2	2
5	Y	77	78	1

The floor vibration was measured in 6 degrees of freedom (DOF) using two Wilcoxon 731A seismic accelerometers. Each can measure acceleration in 1 DOF up to 450 Hz, with a peak of 0.5 g, and two of these combined can be used to measure ground rotational vibration. The measured signal is processed to find the displacement and given as input in DEB-Tool as PSD from 1 Hz to 450 Hz.

The rotational unbalance was modeled with a simple dynamic model, to find the amplitudes of reactions at the stage bearing (point O in Fig. 4(c)) in 6 DOF, given rotation speed ω , mass m_d , height of the center of gravity (COG) h_d , and unbalance distance u_d , as shown in Eq. (1). These amplitudes are then used as a multiplicative factor in DEB-Tool for a PSD of a unitary sine wave at the rotation frequency (Eq. (2)), since the forces will be a single sine with the same frequency as the rotation speed. In the case of using an autobalancing system, the specification is that it will have a mass of up to 70 Hz and will balance the system to 1 N amplitude residual force. To model this into the system, the same approach is used as before, only changing the unbalance distance to result in the 1 N amplitude (Eq. (3)).

$$\begin{cases} F_x = F_z = m_d u_d \omega^2 \\ M_x = M_z = (m_d u_d \omega^2) h + (m_d g) u_d \\ F_y = M_y = 0 \end{cases} \quad (1)$$

$$\text{PSD}_{F_x, \omega} = F_x^2 \text{PSD}(\sin(\omega t)) \quad (2)$$

$$u_{d, \text{auto}} = m_d^{-1} \omega^{-2} \quad (3)$$

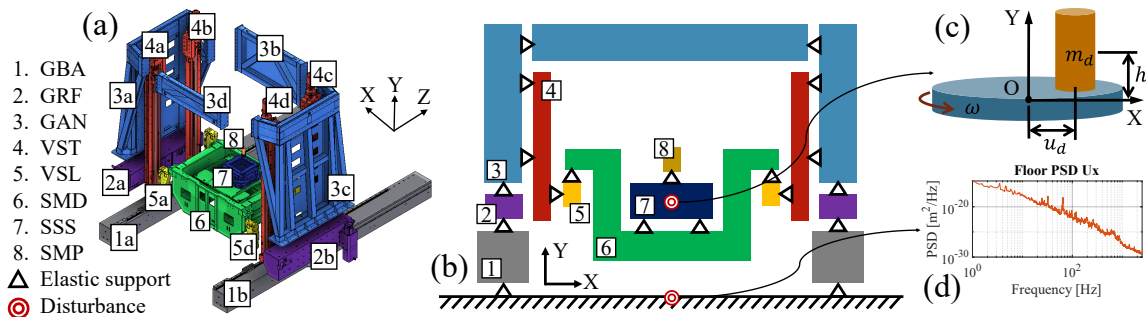


Figure 4: The 3D CAD model, in an exploded view, built in Autodesk Inventor used as input in IET (a). The lumped masses and connections used in DEB-Tool (b). And the modeled disturbances: a dynamic model for rotational unbalance (c), and the measured PSD for the floor vibration (d).

With the input PSD of the disturbances, DEB-Tool uses the dynamic model to output the displacement PSDs, cumulative power spectra (CPSs), or cumulative amplitude spectra (CASSs) at any point of interest (POI) in the model. Here, the POI is the COG of the sample. The result is also divided by contribution: in this case, for each DOF, three curves are output, one for the contribution of the floor, one for the rotational unbalance, and one for the total displacement. Figure 5 shows the output CPS of the sample COG in the X direction with floor vibration and an unbalance of 15 mm of a 40 kg mass rotating at 2 Hz. The contribution of the unbalance to the final vibration is about 40 times larger than the contribution of the floor vibrations on the horizontal direction X, and about 1.5 times on the vertical direction Y.

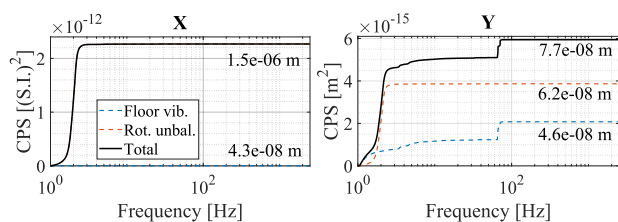


Figure 5: Resulting CPS of sample COG displacement in X (left) and Y (right) directions. The values at the end are the cumulative RMS displacements from each contribution, integrated up to 2.5 kHz.

ERROR BUDGET

Besides the error from the dynamics, the other error that needs to be considered for the microstation is the spindle error motion. Combined, they must total to less than the resolution of the image, which is 500 nm at most. In root mean squared (RMS) terms, the total error of the system must be less than 83 nm RMS on each direction of the image plane (X and Y).

The spindle error motion is a characteristic of the the rotation stage, and it is measured at a spindle error analyzer (SEA) [7]. The measurement is done with loading representative cases: no load at all, to measure the performance of the stage alone; 40 kg load, unbalanced to 20 mm, and rotating at 2 Hz representing the unbalanced system; and 70 kg load, balanced and rotating at 2 Hz, to represent the autobalancing system. The last two cases are the ones used in the error budget. The errors measured with the SEA are on X, Y, Z, Rx, and Rz directions, and these can be manipulated to find the translation of the sample COG, which is at a higher position than the metrology target used in the SEA.

The SEA measurements can be divided into two categories: synchronous (or repeatable) and asynchronous (or random). The synchronous error is the part of the error that repeats every rotation; it is mostly due to the bearing form errors, and can be compensated with metrology and calibration procedures. The asynchronous part is the part that is different every rotation, and can be modeled as random noise; this error can be compensated with in-situ metrology

(that measure the spindle error during the tomography [8]), but not with calibration, as it is not repeatable.

Combining the errors, the error budget for the microstation can be analyzed, and its results are shown in Table 2. The bottom three rows show the combination of all the errors, linearly summed; "with calibration" removes the synchronous error from spindle error motion; and "with metrology" removes the synchronous and asynchronous errors. It is important to note that the calibration and the in-situ metrology would have errors of their own, but based on the stability of our SEA measurement system, that error would be of the order of 10 nm, which is much less than the synchronous error that it would be compensating.

Table 2: Error budget of the microstation. All values in nm RMS. For 500 nm resolution, the total error must be less than 83 nm RMS.

Source	W/o Auto.		W/ Auto.	
	X	Y	X	Y
Dynamics	1500	77	46	46
Spindle sync.	220	85	231	64
Spindle async.	25	27	26	17
Total	1745	189	303	127
W/ calibration	1525	104	72	63
W/ metrology	1500	77	46	46

From these results it can be concluded that the microstation will only be able to perform to its full specifications with the addition of the autobalancing system and at least some calibration. Otherwise, it will be limited to either lower resolutions, lower rotation speeds, or shorter unbalancing distances. Another possibility would be the addition of a metrology system between the floor and the sample, which would be able to compensate the dynamic vibration of the structure, but that seems to be a more expensive and less effective solution than the autobalancing system, as it would probably need high performance metrology at a long distance due to the geometry of the microstation.

CONCLUSION

The dynamics and the disturbances of the microstation have been modeled as a way to help the design process. Here, it was shown how this methodology led to the decision of an autobalancing system, and how the experiments will have to be limited while the autobalancing system is under development.

ACKNOWLEDGMENTS

The authors are grateful for all the support given by our fellow colleagues at LNLS, especially the MOGNO, PLL, OPT, MEP, and MARÉ groups; for the insights from the team at MI-Partners; and also for the funding provided by Petrobras, Equinor, and the Brazilian Ministry of Science, Technology and Innovation.

REFERENCES

- [1] N. L. Archilha *et al.*, “MOGNO, the nano and microtomography beamline at Sirius, the Brazilian synchrotron light source”, *J. Phys.: Conf. Ser.*, vol. 2380, p. 012123, 2022. doi:10.1088/1742-6596/2380/1/012123
- [2] The Pimega 135D 2022, <https://www.pitec.co/pimega-135d>
- [3] R. R. Gerales *et al.*, “Predictive modeling through Dynamic Error Budgeting applied to the High-Dynamic Double-Crystal Monochromator for Sirius light source”, *Precis. Eng.*, vol. 77, pp. 90–103, 2022. doi:10.1016/j.precisioneng.2022.04.009
- [4] R. R. Gerales *et al.*, “Granite Benches for Sirius X-ray Optical Systems”, in *Proc. MEDSI'18*, Paris, France, Jun. 2018, pp. 361–364. doi:10.18429/JACoW-MEDSI2018-THPH12
- [5] A. H. Slocum, “Kinematic couplings: A review of design principles and applications”, *Int. J. Mach. Tools Manuf.*, vol. 50, no. 4, pp. 310–327, 2010. doi:10.1016/j.ijmachtools.2009.10.006
- [6] D. M. Pelt and D. Y. Parkinson, “Ring artifact reduction in synchrotron x-ray tomography through helical acquisition”, *Meas. Sci. Technol.*, vol. 29, p. 034002, 2018. doi:10.1088/1361-6501/aa9dd9
- [7] E. R. Marsh, *Precision spindle metrology*. DEStech Publications, Inc., 2010.
- [8] J. Zhao, “Method for correction of rotation errors in Micro-CT System”, *Nucl. Instrum. Methods Phys. Res. A*, vol. 816, pp. 149–159, 2010. doi:10.1016/j.nima.2016.01.051